Journal of Molecular Liquids 390 (2023) 123047

Contents lists available at ScienceDirect

Journal of Molecular Liquids

journal homepage: www.elsevier.com/locate/molliq

Investigation of the sedimentation characterization of magnetorheological fluids

Roland Nagy [a,*], István Szalai [a,b]

[a] University of Pannonia, Institute of Mechatronics Engineering and Research, Gasparich Márk st. 18/A, Zalaegerszeg, H-8900, Zala, Hungary
[b] University of Pannonia, Research Centre for Engineering Sciences, Mechatronics and Measurement Techniques Research Group, Egyetem st. 10, Veszprém, H-8200, Veszprém, Hungary

ARTICLE INFO

Keywords:
Magnetorheological fluid
Smart fluid
Magnetic suspension
Sedimentation

ABSTRACT

Magnetorheological fluids (MRFs) are smart materials that respond to an external magnetic field by changing their rheological properties. A main drawback of MR fluids is sedimentation which may render the fluids unusable over time. In this study, we introduce a system for the investigation of the sedimentation of magnetorheological fluids in the gravitational field. First of all, differential equation approximations describing the initial stage and the post-saturated stage of the sedimentation are proposed to correlate the experimental results. The custom-developed apparatus is explained, which incorporates a measuring sensor with a lock-in amplifier, a vertically positioned test tube, and a motorized z-axis translating stage. The measurement principle is based on the change of mutual induction between the primary and secondary coils of a sensor, according to the volume fraction-dependent susceptibility. The sensor's coils are driven by a lock-in amplifier, which is able to sense the minor settling distances. The motorized translating axis provides the opportunity for the analysis of the concentration profile of the sample column along its entire length and the device is able to work in fully automated mode. The performance of the device is validated by measurements with Lord MR fluids, for which the sedimentation constant and ratio metrics are provided.

1. Introduction

Magnetorheological fluids are suspensions of micron-sized magnetic particles in a non-magnetic liquid medium such as silicone oil. The typical MR fluids contain 30-40 volume percent of ferro- or ferrimagnetic spherical particles, carrier fluid, and additives. The viscosity and shear stress of the suspension can be controlled by varying the strength of the external applied magnetic field. If there is no external magnetic field (off-state) the viscosity of MR fluids depends mainly on the fraction of the solid particles, the viscosity of the carries fluid, and the possible additives. While under an external magnetic field (on-state) the viscosity depends mainly on solid particle fraction, magnetic field strength, and saturation magnetization of the particles [1] [2]. MRFs have gained wide application as semi-active vibration absorbing systems and vehicle suspensions, furthermore in aircraft utilizations too [3].

1.1. MR fluid behavior

Conventional magnetorheological fluids utilize ferromagnetic particles which have diameters around 1-10 μm. The most used materials are iron and magnetite, these have high saturation magnetization attribution. This is important because the higher the saturation magnetization is, the higher the maximum yield stress will be. The micron-sized particles have multiple magnetic domains. In off-state, each domain has its own magnetic moment, but the orientation of the moments are different and they cancel each other out, so the particles of an MR fluid have no net magnetization. In on-state, the domain's magnetic moment will be parallel to the external magnetic field and there will be only one domain within the particle. Consequently, the particles acquire a magnetic polarization and attract one another forming chain-like structures that join to form columnar structures. The newly formed structure has increased viscosity and apparent yield stress under shear [4] [5] [6].

1.2. Off-state properties

In the absence of an external magnetic field, the magnetic particles are randomly distributed in the carrier fluid and the forces they encounter are mostly hydrodynamic. Due to the dominant force being the gravitational force the magnetic particles settle in the MR fluid after

* Corresponding author.
E-mail addresses: nagy.roland@mk.uni-pannon.hu (R. Nagy), szalai.istvan@mk.uni-pannon.hu (I. Szalai).

https://doi.org/10.1016/j.molliq.2023.123047
Received 15 May 2023; Received in revised form 16 August 2023; Accepted 9 September 2023
Available online 17 September 2023

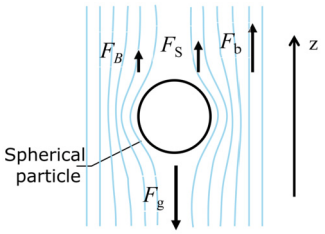

Fig. 1. Schematic diagram of the forces acting on a settling spherical particle.

remixing. Sedimentation is mainly influenced by the density mismatch between the particles and the carrier fluid [7]. The net force (F_{net}), that is acting on a single spherical particle in a fluid medium is given as

$$F_{\text{net}} = F_g - F_b - F_S - F_B \tag{1}$$

where F_g is the gravitational force, F_b is the buoyancy force, F_S is the Stokes force, and F_B is the Brownian force, which are shown in Fig. 1. From Eq. (1) the gravitational force, that acting on a spherical particle is defined as

$$F_g = \frac{4}{3} r^3 \pi \rho_p g \tag{2}$$

where r is the radius of the particle, ρ_p is the density of the particle and g is the gravitational acceleration. The buoyancy force is in the opposite direction to the gravitational force and it defined as

$$F_b = \frac{4}{3} r^3 \pi \rho_f g \tag{3}$$

where ρ_f is the density of the carrier fluid. The Stokes force is also opposed by the gravitational force, which describes the fluid resistance force acting on a slowly moving body in a fluid:

$$F_S = 6\pi\eta r v \tag{4}$$

where η is the apparent viscosity of the carrier fluid and v is the velocity of a single particle. The Brownian forces (F_B) result from the random thermal movement of carrier fluid molecules that are colliding with particles, which are generally opposed to the gravimetric forces [1] [8]. However, [9] says that these weak forces are negligible and are therefore not considered further.

Conventionally, the role of the particle-particle interactions during dispersion sedimentation can be investigated with good accuracy by simulation techniques [9]. The single-particle approximation is thus a rough model to describe the sedimentation of a dispersion, but using solutions of the differential equation, functions can be proposed to correlate the measurement results.

(a) Initial stage

On the basis of Newton II. law, the equation of motion at the initial stage of sedimentation:

$$\frac{dv}{dt} + \beta v = \alpha, \tag{5}$$

where $\alpha = \left(1 - \frac{\rho_f}{\rho_p}\right) g$ and $\beta = \frac{9}{2} \frac{\eta}{r^2 \rho_p}$, with the initial condition $v(t=0) = 0$. By solving analytically the ordinary differential equation of Eq. (5) we obtain the settling velocity of an immersed, single-sphere shape particle until the saturation point

$$v = \frac{\alpha}{\beta}(1 - e^{-\beta t}) \tag{6}$$

Thus, a function $y_1(t) = a(1 - e^{-bt})$ can be fitted to the initial part of the sedimentation curve. This simplified model is particularly useful in the early stages of sedimentation, as the particles that are sedimenting become more inhibited as time increases, thereby reducing the sedimentation rate.

(b) Post-saturation stage

The magnetic particles will settle if the gravitational force is larger than the buoyancy and Stokes forces together. The downward movement of a particle requires upward back-flow of the carrier fluid during sedimentation. Because the flow of the carrier fluid is hindered if the viscosity of the carrier fluid or the number of the neighboring particles increases the sedimentation process will slow down over time. The time at which the sedimentation rate starts to decrease is called the saturation point [10] [11].

To describe this phenomenon, we propose the steps following for the decreasing velocity stage. Brenner [12] proposes a correction factor of $f = 1 + \frac{9}{8}\frac{r}{h}$ to consider the bottom effect, but this is only applicable to small Reynolds numbers. According to Brenner, we propose the function of $f = \frac{h_0}{h}$, as it takes a stronger effect into account. Thereby, the original differential equation (Eq. (5)) is modified to

$$\frac{dv}{dt} + \beta f v = \alpha. \tag{7}$$

In the constant velocity range, we assume that $\frac{dv}{dt} \approx 0$, therefore

$$v = \frac{\alpha}{\beta h_0} h. \tag{8}$$

Whereas the direction of velocity and displacement are opposite,

$$-\frac{dh}{dt} = v. \tag{9}$$

Finally, we obtain the differential equation of

$$\frac{dh}{dt} + \frac{\alpha}{\beta h_0} h = 0, \tag{10}$$

with initial condition of $h(t=0) = h_0$. From its solution, for the velocity we obtain

$$v = \frac{\alpha}{\beta} e^{-\frac{\alpha}{\beta h_0} t}, \tag{11}$$

which justifies fitting a curve of type $y_2(t) = ce^{-dt}$ in the saturated section.

Various strategies have been used to reduce sedimentation velocity. One of them is the use of nanoparticles, with an average diameter of 10-100 nm. Nevertheless, if the suspension homogeneity is lost due to sedimentation, the MR fluid is no longer effective. In practical engineering applications, already when stratification occurs, the performance of MR devices may be compromised, especially in cases where the MR device is used infrequently such as in earthquake dampers [13] [14].

1.3. Methods for sedimentation monitoring

Several studies have been carried out recently on the sedimentation of suspensions containing magnetic particles. Silfhout et al. [15] and Luigjes et al. [16], used a practical approach to characterize the sedimentation rate and concentration profile of ferrofluids with magnetic particles. In their studies, custom-prepared fluids were investigated, allowing detailed theoretical modeling, while sedimentation characteristic measurements were carried out by measuring the magnetic field as a function of sample column height using a Hall probe. Silfhout and Erne, [17] investigated the sedimentation rate of fluids with magnetic particles using X-ray transmission profiles measurement. Furthermore, the effects of specific factors on sedimentation, such as particle concentration and viscosity, were investigated. Xie et al., [18] used an inductance-based method to investigate the sedimentation stability of magnetorheological fluids. The measurement system was constructed to measure the particle concentration at several points of a vertical column of the fluid sample, with a total measurement time of 96 days, considering the low rate of the sedimentation process. In their study, they highlighted the role of the fact that the composition of the settling suspension in the tube has four zones. The most-upper zone is a clear fluid layer, that does not contain magnetic particles. Below this is the original

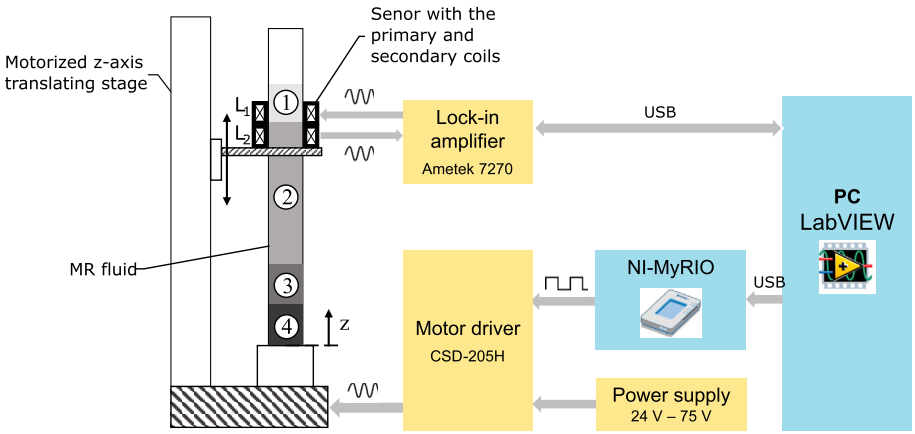

Fig. 2. Schematic of the automated vertical axis measuring device. The following phases can be observed in the fluid column: ① upper clear fluid layer, ② original concentration zone, ③ variable concentration zone, ④ sediment zone.

concentration zone, the variable concentration zone and the lowermost is the sediment zone. As solid particles saturate sections of the fluid column by settling, thus layers of constant concentration appear to propagate upwards. This does not mean that solids are propagating upwards, merely giving rise to lines called concentration characteristics [19] [20]. The boundary between the clear fluid layer and the original concentration zone is called mudline, from the change in position and time can be obtained the sedimentation rate of the suspension. Cheng et al., [21] used a novel thermal conductivity monitoring approach to measure the sedimentation rate of magnetorheological fluids. In their study, a linear relationship between the particle concentration and thermal conductivities was observed. A series of MRFs were prepared and tested, however, the measurement duration was only 17 h.

Pshenichnikov et al., [22] [23] applied Monte Carlo method and molecular dynamics approach to study the gravitational sedimentation of magnetic particles. They have achieved remarkable results, but the theoretically based approach and modeling of magnetic suspensions is a complex process, as the effects of many variables have to be considered. These equations take into account steric, magnetodipole, and hydrodynamic interparticle interactions, however, the development of a more elaborate model poses the risk of overinterpretation [17]. Furthermore, in many cases, the exact composition of the fluids is not known, which would be necessary for modeling. For these reasons, the measurement-based investigation of the sedimentation of these fluids is of high importance.

Therefore, the objective of this study is to design and build an apparatus that can be used to investigate the sedimentation velocity of conventional magnetorheological fluids. An essential aspect is that the apparatus should be able to detect the concentration changes throughout the entire length of the fluid sample, and the objective is to achieve a simple and low-cost device without the need for complex sensors.

2. Automated vertical axis measuring device

The automated vertical axis measuring device's working principle is shown in Fig. 2. The sensor unit of the apparatus consists of two windings, which are based on the principle of mutual inductance to detect the change of volume fraction of solid particles at a given height. The module is connected to the control PC via a lock-in amplifier. A long cylindrical test tube is placed inside the measuring coil's air gap. The test tube contains the magnetorheological fluid sample. The test tube's inner diameter is 3 mm and the length is 400 mm. With attention to the diameter of the test tube, the walls of the container have no effect on the rate of sedimentation if the ratio of the diameter of the vessel to the diameter of the particle is greater than about 100 [24]. Along with this if the walls of the container are vertical, and therefore the cross-sectional area does not vary with depth, the shape of the container has little effect on the sedimentation rate.

The sensor contains a primary (L_1) and a secondary (L_2) winding in a close-together arrangement. The primary coil is excited by the output of the lock-in amplifier, and the ferromagnetic particles in the MR fluid sample act as an iron core, therefore the primary and secondary winding is magnetically linked together and mutual inductance induces a voltage in the secondary coil. Due to the coupling between coils, the induced voltage is highly dependent on the volume fraction of magnetic particles at the current cross-section according to the altitude-dependent susceptibility. The relationship between particle concentration and susceptibility can be derived as shown below. First, start from the Maxwell-Garnett equation expressing the magnetic permeability (μ) of a monodisperse MR fluid:

$$\frac{\mu-\mu_b}{\mu+2\mu_b}=\varphi\frac{\mu_p-\mu_b}{\mu_p+2\mu_b} \tag{12}$$

where μ_b is the permeability of the carrier fluid, μ_p is the permeability of the magnetic particles and φ is the volume fraction. Moving from permeability to susceptibility in terms of $\chi=\mu-1$, it can be written that

$$\chi=\varphi\frac{3\chi_p}{3+\chi_p(1-\varphi)} \tag{13}$$

For small φ this equation was linearized by Gorodkin et al. [25] as follows and the notation is introduced:

$$\chi=\chi_s\varphi \tag{14}$$

where $\chi_s=\frac{3\chi_p}{3+\chi_p}$ and χ_s is the slope of the χ vs. φ curve. Their results show that for carbonyl-iron based particles the slope of χ_s varies between 1.77 and 8.03 and the linear equation correlates well with our experimental data. At different dilutions, the linear relation was verified for our MR fluid samples by measurements. In our case, the value of χ_s ranges between 5 and 6, which is consistent with the data of Gorodkin et al. [25]. This means that the induced voltage in the coil is proportional with χ and according to Eq. (14) linearly depends on the volume fraction. The secondary winding's signal is processed by the lock-in amplifier (Ametek 7270 DSP). The lock-in amplifier amplifies only the given frequency signal, this allows accurate measurement with approximate suppression of external noise. Furthermore, due to the exciting voltage's amplitude and frequency can be varied, the sensitivity of the sensor can be adjusted to the MR fluid properties. During our measurements, the excitation frequency was set to 700 Hz and the amplitude to 3 V, since this configuration showed the highest sensitivity.

Due to the settling time can take several months, thereby it is necessary to measure many times, so a fully automatic measuring device was

Table 1
Composition of MR fluid samples.

Type of MR fluid	MRF-140CG	MRF-122EG
Solids content by weight	85 m/m%	72 m/m%
Apparent viscosity	0.280 Pa-s	0.042 Pa-s
Density of MR fluid	3.5-3.7 g/cm^3	2.2-2.4 g/cm^3
Range of particle diameter	2 - 10 μm	2 - 10 μm

designed. The sensor is translated along the vertical axis by a motorized linear unit and the measurement data will be automatically saved to the computer. The measurement period time can be set before the MR sample fill-in process. Furthermore, the sensor stage velocity, the measurement height, and the lock-in amplifier settings can be set from the apparatus's program on the computer. The controller unit (MyRIO-1900-National Instruments) is responsible for the data acquisition, the communication between the units, and the control of the motorized linear unit. Thereby, the long-time measurements can be easily executed by the automated measuring device.

The sensor stage can move along the whole height of the test tube, therefore, the entire sedimentation characterization can be observed. The described automated vertical axis measuring device and method has been validated by measurements on commercially available magnetorheological fluids.

3. Results and discussion

In this study, two commercially available MR fluid samples were studied by the automated measuring device. Each of the samples was made by the Lord company and both of them contain iron microparticles with a diameter of range 2 and 10 μm, and the matrix is polydimethylsiloxane. One of the measured fluid types was the MRF-140CG, while the type of MRF-122EG MRF was used for comparison. Both of the used MR fluid composition is shown in Table 1.

3.1. Measurement setup

The magnetorheological fluid samples were prepared by manually mixing. A syringe was used to vacuum the MR fluid into the test tube from the bottom of the tube to avoid air bubbles. The samples were kept maintained at room temperature for 24 hours before the measurements to equilibrate temperature. Furthermore, during this initial period, the effects of filling the test tube can still have an influence on the movement of the particles. The height of the initial fluid column was 330 mm with the MRF-140CG, and 275 mm with the MRF-122EG. According to [24] the height of suspension does not generally affect the sedimentation rate. Previous studies recommended the length of the measurement period should be as extended as possible, as this can help to better understand the sedimentation process. Furthermore, the sedimentation rate can vary significantly between different time sections [2]. The measurement interval was 70 days and the measurements were carried out every day by the automated mode of the device, without human intervention.

3.2. Raw measurement results

After the measuring period, the experimental data are summarized in Fig. 3 for the type of MRF-140CG and Fig. 4 for the MRF-122EG, where 10^5 sec ≈ 1 day. The figures show the raw output voltage of the lock-in amplifier unit as a function of time and height. The bottom of the test tube is the reference altitude (0 mm). As shown in Fig. 3, the original induced voltage value is very stable throughout the measurement period for the MRF-140CG sample. With time, the induced voltage at the bottom of the sample column slowly increased with the increasing volume fraction of particles. At the top of the column, the variable concentration zone began to form continuously from day 10. As shown

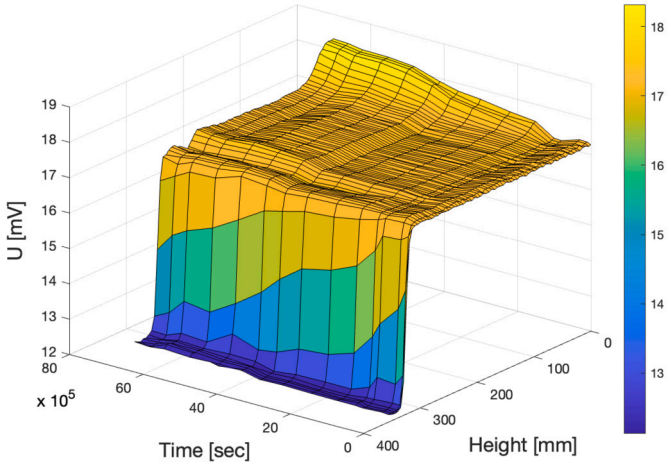

Fig. 3. The effective value of measured voltage as a function of time and height for MRF140CG (10^5 sec ≈ 1 day).

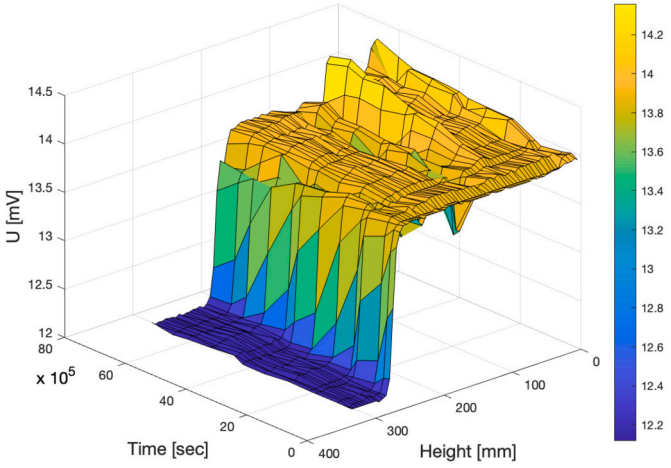

Fig. 4. The effective value of measured voltage as a function of time and height for MRF122EG (10^5 sec ≈ 1 day).

in Fig. 4 on the last measured data curves the different concentration zones formed as mentioned previously. In height of between 70 mm and 170 mm, the variable concentration zone, between 170 mm and 235 mm the original concentration zone, and the gap between the initial state and the 70 days state (275 mm and 235 mm) presents the clear fluid layer. As can be seen, at the bottom of the test tube the volume fraction of the particles is continuously increasing as in the sample of MRF140CG. The difference between the formed concentration zones of each sample derives from the various apparent viscosity. Since the MRF-122EG fluid has a significantly lower viscosity when the particles settle downwards the carrier fluid can flow up with less resistance. As a result, the different concentration zones appear more decisively and they are clearly manifesting themselves than in sample MRF-140CG. The difference in the volume fraction of particles between the two samples is noticeable from the basic value of induced voltage.

Fig. 5 focuses only on the top of the fluid column. The vertical axis indicates the measured voltage and the horizontal axis indicates the height of the fluid column on both (a) and (b) figures. As the figures show measurement data for several days, it indicates the position change of the mudline. According to this, the entire mudline travel is about 10 mm for MRF-140CG. Since the MRF-122EG fluid's apparent viscosity is significantly less and it has fewer particles in the same volume, thus the mudline travel here is about 35 mm.

The particles in the MR fluid column tend to sink to the bottom of the column if the gravity force is larger than the others. As the parti-

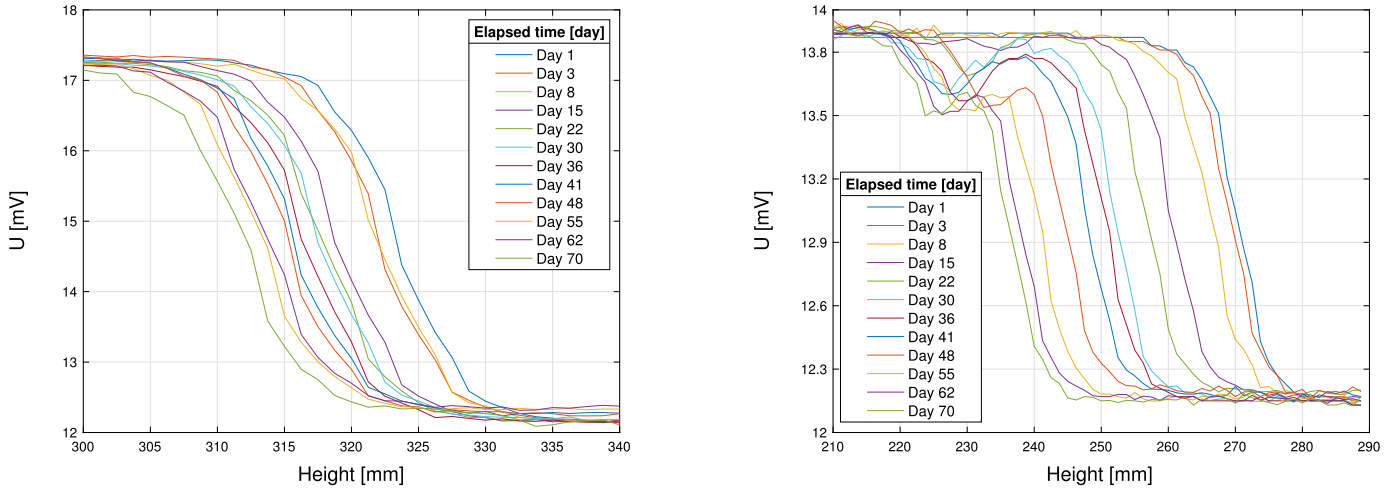

(a) MRF140CG (b) MRF122EG

Fig. 5. Changing of the induced voltage as a function of height over time at the top of the MRF column, see also the change of the mudline position.

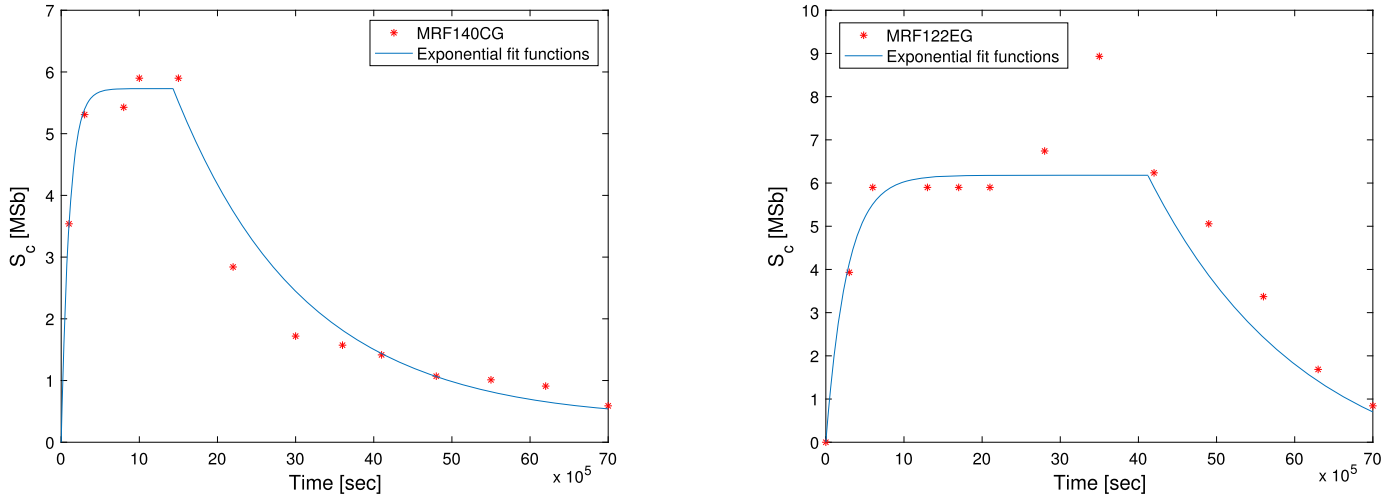

(a) MRF140CG (b) MRF122EG

Fig. 6. Sedimentation constant according to time sections as a function of time.

cles sink to the bottom, a layer of clear fluid forms at the top of the column from the carrier fluid. The boundary between the supernatant zone and the concentrated MRF, the mudline can be observed visually if the carrier fluid is translucent. In this study, the height of the supernatant zone and the entire fluid column can be defined by the data of Fig. 5a for MRF-140CG and Fig. 5b for MRF-122EG, showing the change of mudline height as a function of time at the top of the fluid column.

3.3. Derived metrics

The sedimentation velocity (v, sedimentation rate) is defined as the rate at which the mudline sinks due to particle settling until the particles get down to the bottom of the test tube without further sedimentation. Since the net force acting on the particles can vary depending on the measurement system, therefore the sedimentation rate of the solid particles is commonly expressed by the sedimentation constant, S_c. The sedimentation constant is the ratio of the sedimentation rate and the value of acceleration, under gravity $g = 9.81$ m/s^2:

$$S_c = \frac{v}{g} \tag{15}$$

The sedimentation constant's unit is Svedberg, which is a measure of time, defined as 1 Sb= 10^{-13} s. For magnetorheological fluids, the Svedberg unit is fairly low, so the megaSvedbergs are usually used. Since the sedimentation rate changes over time due to particle-particle interaction and as the suspension saturates, therefore the settling constant is calculated as a function of time. Fig. 6a shows the sedimentation constants according to time sections to the entire measuring time for MRF-140CG and Fig. 6b for MRF-122EG. As shown in Fig. 6a the sedimentation constant for the initial state is $3.5 \cdot 10^{-4}$ MSb, 10 days later it is close to $6 \cdot 10^{-4}$ MSb. In the further time sections of the measurement, the sedimentation constant continuously decreases up to $0.7 \cdot 10^{-4}$ MSb. For MRF-122EG, the initial sedimentation constant is $4 \cdot 10^{-4}$ MSb, afterward 6 days it is $6 \cdot 10^{-4}$ MSb. The sedimentation constant is growing up to $9 \cdot 10^{-4}$ MSb. By the decreasing of the sedimentation velocity, the sedimentation constant sharp decreases too, up to $1 \cdot 10^{-4}$ MSb.

To correlate the measurement data, exponential type functions were fitted according to Subsection 1.2. Separately for the initial stage a $y_1(t)$ type function (see Eq. (6)) and for the post-saturation stage a $y_2(t)$ type function (see Eq. (11)) have been fitted. One measure of goodness of fit is the coefficient of determination or R-squared value, which indicates how closely the values that obtained from fitting match with the

original values. The average R-squared value is 0.94 for the MRF140CG fluid and 0.97 for the MRF122EG sample. Furthermore, the character and transition between the initial and the post-saturation phase can be well observed by the fits. Thereby, it can be noted that the initial stage duration of MRF122EG is more than twice that of MRF140CG, which can be related to the later saturation due to the lower solid particle content.

A further important measure of sedimentation is the sedimentation ratio, which is defined as the volume of the clear fluid layer above the mudline, and the volume of the entire suspension [26]. By using standard test tubes, the shape of the cross-section is the same throughout the whole height. Therefore, the sedimentation ratio, $R(t)$ is the ratio of the height of the clear fluid layer, $h_{\text{supernatant}}$, to the total height of the fluid column, H_{entire}, as shown by Fig. 7. These values were determined on the basis of Fig. 5a for MRF-140CG and Fig. 5b for MRF-122EG. Furthermore, the exact value of H_{entire} was obtained from the lower initial increase point of the mudline curve instead of the inflection point, as in our experience the sensor provides the most reliable reference point at this level. The percentage of sedimentation ratio for MRF-140CG is plotted as a function of time in Fig. 8a. As shown, the sedimentation ratio is continuously increasing up to 3%. Fig. 8b shows the sedimentation ratio for MRF-122EG, which is growing approximately linearly up to 11% during the 70 days measuring period. The slope of the sedimentation ratio curve also shows the trend in the sedimentation velocity. According to this, can be noticed from both figures that the initial sedimentation rate is lower than the average sedimentation rate, which is supported by [21] reference's experiences. The maximum sedimentation rate was in between 10 and 20 days for MRF-140CG and between 30 and 40 days for MRF-122EG. From day 45 the sedimentation velocity is continuously decreasing until day 65, where the sedimentation velocity is approximately zero. In Fig. 8a (MRF-140CG), a more linear sedimentation rate is noticeable, which is caused by the higher viscosity of the MR fluid. To obtain the type of the fitting function for the sedimentation ratio values, the integral of the exponential functions ($y_1(t), y_2(t)$) fitted to the sedimentation constant values (Fig. 6) were used. The R-squared value for the MRF140CG sample is 0.89 and 0.8 for the MRF122EG fluid.

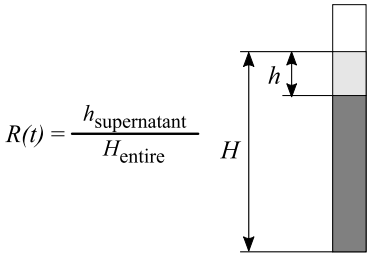

Fig. 7. Illustration of sedimentation ratio.

3.4. Validation

There are limited possibilities to validate the results by comparison, as there is no universally accepted or standardized measurement procedure for the sedimentation of magnetorheological fluids [5]. Therefore, the measurement and evaluation methods and measurement times described in the literature vary considerably. Furthermore, many measurements have been carried out for significantly shorter periods of time, which makes it difficult to compare long-term measurement results [2]. Lord-type magnetorheological fluid was investigated by Xie et al. [18], however, the MRF126CD-type suspension they investigated is no longer commercially available, but has properties close to MRF122EG fluid. Results were reported at regular intervals for the first 28 days and then at day 96. The sedimentation ratio was approximately 8% on day 28 and 15% on day 96 at comparable measurement time points. Furthermore, the results summarized in the review article provided by Kumar et al. [6] reflect that these types of fluids generally show a sedimentation ratio of a few percent over a 3-month period. Furthermore, the characteristics of the sedimentation velocity and ratio curves given by Holdich [19] and Alapati [11] are in good agreement with the presented measurement results. In addition, changes in mudline travel were visually monitored during the measurements, which was consistent with the results provided by the apparatus.

4. Conclusion

In this study, a measuring device has been designed and built to measure the sedimentation characterization of magnetorheological fluids. The device incorporates a motorized vertical axis translating stage on it with the sensor unit, due to this the apparatus is able to work in fully automatic mode on its own. The measuring device has been experimentally validated by measurements on commercially available magnetorheological fluids, by Lord MRF-140CG and Lord MRF-122EG. The measurement has been carried out for 70 days with a measurement taken every day. The measurements were performed in fully automatic mode without human intervention. In the sample columns, the volume fraction of the magnetic particles changed as a function of time and as

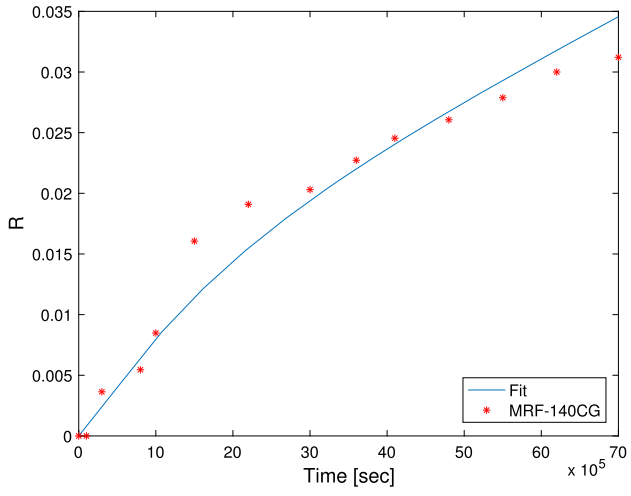

(a) MRF140CG

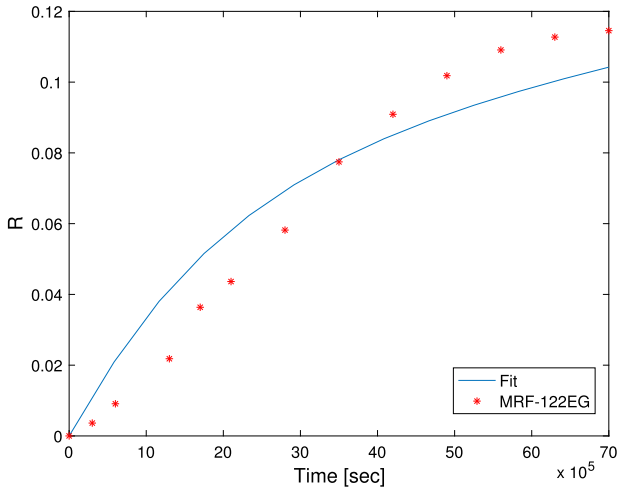

(b) MRF122EG

Fig. 8. Sedimentation ratio as a function of time.

a function of height. The sedimentation velocity has been determined from the mudline travel, which is $v = 1.4$ nm/s for MRF-140CG and $v = 5.8$ nm/s for MRF-122EG for the measurement interval. From there, the average sedimentation constant has been computed (see Eq. (15)), what is $S_c = 2.82 \cdot 10^{-4}$ MSb for MRF-140CG and $S_c = 7.24 \cdot 10^{-4}$ MSb for MRF-122EG. The maximum sedimentation ratio at the end of the measurement period was 3% for MRF-140CG and 11% for MRF-122EG. Based on previous experience, the measurements were carried out over a considerable period of 70 days, which helped to understand the settling process in more detail. The measurement results were compared with the available literature data, which are in agreement and our visual inspections for the visible mudline settling range. Due to the automatic mode, these long-time measurements were simple to execute, although the time required for measurements is still significant. To address this problem, a centrifuge-based system is being developed that would significantly speed up the start-to-finish process. These methods will also be published in the future.

Declaration of competing interest

The authors declare that they have no known competing financial interests or personal relationships that could have appeared to influence the work reported in this paper.

Data availability

Data will be made available on request.

Acknowledgements

The research was supported by European Union and co-financed by the European Social Fund. EFOP-3.6.2-16-2017-00002

References

[1] I. Jonkkari, Rheological characterization of magnetorheological fluids, 1566, Tampere University of Technology, 2018, pp. 3–56.
[2] D.Y. Chen, L.S. Chen, Permalloy inductor based instrument that measures the sedimentation constant of magnetorheological fluids, AIP Publishing, Rev. Sci. Instrum. 74 (7) (2003) 3566–3567.
[3] N.M. Wereley, T. Ngatu, Viscometric and sedimentation characterization of bidisperse magnetorheological fluids, IEEE Trans. Magn. 43 (6) (2007) 2474–2476.
[4] N.M. Wereley, R.C. Bell, D.T. Zimmerman, Impact of Nanowires on the Properties of Magnetorheological Fluids and Elastomer Composites, The Pennsylvania State University, 2010, pp. 190–210.
[5] M. Ashtiani, S.H. Hashemabadi, A. Ghaffari, A review on the magnetorheological fluid preparation and stabilization, J. Magn. Magn. Mater. 374 (2015) 716–730.
[6] J.S. Kumar, P.S. Paul, G. Raghunathan, D.G. Alex, A review of challenges and solutions in the preparation and use of magnetorheological fluids, Int. J. Mech. Mater. Eng. 14 (2019) 1–18.
[7] H. Eshgarf, A.A. Nadooshan, A. Raisi, An overview on properties and applications of magnetorheological fluids: dampers, batteries, valves and brakes, J. Energy Storage 50 (2022) 104648.
[8] A.P. Philipse, Colloidal sedimentation and filtration, Curr. Opin. Colloid Interface Sci. 2 (2) (1997) 200–206.
[9] K.J. Son, A discrete element model for the influence of surfactants on sedimentation characteristics of magnetorheological fluids, Korea-Australia Rheol. J. 30 (1) (2018) 29–39.
[10] T. Hagemeier, D. Thévenin, T. Richter, Settling of spherical articles in the transitional regime, Int. J. Multiph. Flow 138 (2021) 103589.
[11] S. Alapati, W.S. Che, Y.K. Suh, Simulation of sedimentation of a sphere in a viscous fluid using the lattice Boltzmann method combined with the smoothed profile method, Adv. Mech. Eng. 7 (2) (2015).
[12] H. Brenner, The slow motion of a sphere through a viscous fluid towards a plane surface, Chem. Eng. Sci. 16 (1961) 242–251.
[13] P.Y. Lin, T.K. Lin, Control of seismically isolated bridges by magnetorheological dampers and a rolling pendulum system, Struct. Control Health Monit. 19 (2011) 278.
[14] N.M. Rahbari, B.F. Azar, S. Talatahari, H. Safari, Semi-active direct control method for seismic alleviation of structures using MR dampers, Struct. Control Health Monit. 20 (2012) 1021.
[15] A.M. van Silfhout, H. Engelkamp, B.H. Erne, Magnetic sedimentation velocities and equilibria in dilute aqueous ferrofluids, J. Phys. Chem. 124 (2020) 7989–7998.
[16] B. Luigjes, D.M.E. Thies-Weesie, A.P. Philipse, B.H. Erne, Sedimentation equilibria of ferrofluids: I. Analytical centrifugation in ultrathin glass capillaries, J. Phys. Condens. Matter 24 (24) (2012) 245103.
[17] A.M. van Silfhout, B.H. Erne, Magnetic detection of nanoparticle sedimentation in magnetized ferrofluids, J. Magn. Magn. Mater. 472 (2019) 53–58.
[18] L. Xie, Y.T. Choi, C.R. Liao, N.M. Wereley, Characterization of stratification for an opaque highly stable magnetorheological fluid using vertical axis inductance monitoring system, AIP Publishing, J. Appl. Phys. 117 (2015) 17C754.
[19] R.G. Holdich, Fundamentals of Particle Technology, Midland Publishing, 2002, pp. 43–76.
[20] G.J. Kynch, A theory of sedimentation, Trans. Faraday Soc. 48 (1952) 166–176.
[21] H. Cheng, X. Zhang, G. Liu, W. Ma, N.M. Wereley, Measuring the sedimentation rate in a magnetorheological fluid column via thermal conductivity monitoring, IOP Publishing, Smart Mater. Struct. 25 (2016) 5.
[22] A.F. Pshenichnikov, E.A. Elfimova, A.O. Ivanov, Magnetophoresis, sedimentation, and diffusion of particles in concentrated magnetic fluids, J. Chem. Phys. 134 (18) (2011) 184508.
[23] A.F. Pshenichnikov, A.A. Kuznetsov, Sedimentation of particles in concentrated magnetic fluids: numerical simulation, Magnetohydrodynamics 51 (3) (2015) 551–560.
[24] B. Gurappa, R.P. Chhabra, Coulson and Richardson's Chemical Engineering, Particulate Systems and Particle Technology, vol. 2a, Butterworth-Heinemann, 2018.
[25] S.R. Gorodkin, R.O. James, W.I. Kordonski, Magnetic properties of carbonyl iron particles in magnetorheological fluids, J. Phys. Conf. Ser. 149 (2009) 012051.
[26] H.B. Cheng, J.M. Wang, Q.J. Zhang, N.M. Wereley, Preparation of composite magnetic particles and aqueous magnetorheological fluids, IOP Publishing, Smart Mater. Struct. 18 (2009) 2–6.